Case Studies in Construction Materials 21 (2024) e03971

Contents lists available at ScienceDirect

Case Studies in Construction Materials

journal homepage: www.elsevier.com/locate/cscm

New impulse-based test method for early-age elastic modulus measurement in cementitious materials

Amir Araghi [a,*], Renan Rocha Ribeiro [b], Thomas Russo [b], José Granja [b], Miguel Azenha [b], Rodrigo de Melo Lameiras [a]

[a] Universidade de Brasília, Departamento de Engenharia Civil e Ambiental, Brasília, Brazil
[b] University of Minho, ISISE, ARISE, Department of Civil Engineering, Guimarães, Portugal

ARTICLE INFO

Keywords:
Elastic modulus
EMM-ARM
Open-source
Low-cost
Impulse-based sample excitation
Mechanical properties

ABSTRACT

Accurate monitoring of the elastic modulus evolution during the early-age fluid-solid transition in cementitious materials is crucial for understanding their mechanical behavior under early stresses. While existing methods, such as EMM-ARM, have proven effective, they are often associated with high costs or complex setups. This study presents the development of a low-cost, easy-to-implement system that employs impulse excitation applied to a composite beam, introducing the EMM-IRM method for the effective assessment of the elastic modulus of cement paste from the earliest stages of hydration. The use of impulse excitation is particularly advantageous in low-cost systems with accelerometers of lower sensitivity, as it enhances signal clarity and reduces interference from background noise, thereby improving measurement reliability. The system was validated through experimental comparisons with conventional EMM-ARM, cyclic compression, and traditional impulse excitation techniques, using Portland cement paste as the test material. The results show that EMM-IRM consistently estimates the elastic modulus, with a maximum deviation of 6.33 % from other methods. Moreover, despite its cost-effectiveness, EMM-IRM demonstrates a higher signal-to-noise ratio compared to conventional EMM-ARM. This approach offers a practical solution for early-age characterization of cementitious materials, balancing cost, simplicity, and measurement accuracy.

1. Introduction

Extensive research endeavors are being pursued with the primary objective of mitigating the environmental impact associated with cement-based materials. This pursuit encompasses the development of novel materials, including the exploration of new fillers, alternative waste constituents for incorporation, and materials that demand reduced energy inputs during their production [1]. In light of the introduction of these novel materials, a critical imperative arises for rigorous testing procedures aimed at comprehensive characterization of their mechanical properties prior to their practical deployment.

Within the various stages of the mechanical property evolution of these new cement-based materials, characterizing the early stages of development is of paramount importance. This knowledge enables the assessment of how cementitious materials perform under the stresses they experience during their early development. These stresses can result from volumetric changes caused by heat generated during hydration, autogenous shrinkage deformations, or early loading, such as pre-stress application and the removal of

* Corresponding author.
E-mail address: amirmahdiaraghi74@gmail.com (A. Araghi).

https://doi.org/10.1016/j.cscm.2024.e03971
Received 16 August 2024; Received in revised form 17 October 2024; Accepted 7 November 2024
Available online 8 November 2024

formwork or propping [2].

It has been about a decade since a methodology known as Elasticity Modulus Measurement through Ambient Response Method (EMM-ARM) was developed and optimized to monitor the elastic modulus evolution of cementitious materials, as well as other materials undergoing fluid-solid hardening transitions, from their earliest age [2–20]. This method is a variant of the resonant frequency techniques [21,22], adapted for early-age investigations. It utilizes ambient noise (e.g., noises from a construction site, voices, wind, etc.), which can be conceptualized as white noise, as excitation for measuring the vibration frequency of a composite beam composed of a mold filled with the material under investigation [2,4]. Previous studies have revealed that EMM-ARM yields an elastic modulus measurement that closely approximates the static modulus [12], in contrast to the dynamic modulus commonly obtained through resonant frequency methods [2,4,23,24].

The original EMM-ARM test system [2,4,12,14] relies on commercially available general-purpose data-acquisition systems and accelerometers. Besides incurring non-negligible costs and being dependent on proprietary platforms [25], these components require rather specialized knowledge to adapt and configure for executing measurements in accordance with the EMM-ARM method [26]. To address these challenges, Ribeiro et al. [26] proposed a cost-effective microcontroller-based test system tailored for cement paste EMM-ARM experiments, which also uses ambient noise excitation. While this low-cost system demonstrated promising results

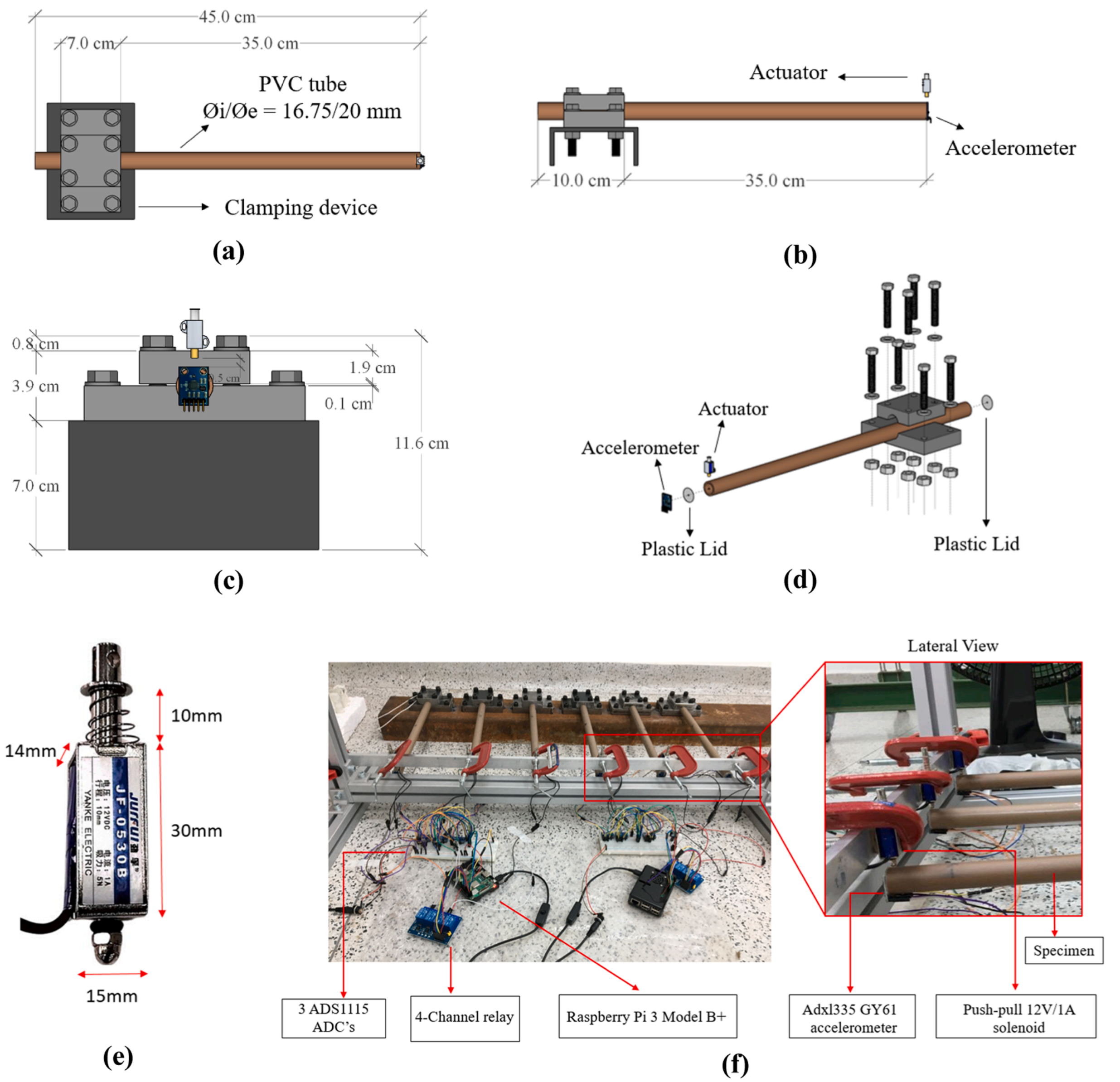

Fig. 1. Scheme of the physical setup: **(a)** Top view; **(b)** Front view; **(c)** Lateral view; **(d)** 3D exploded view; **(e)** Actuator dimensions; **(f)** Real test setup.

compared to the original setup, it also exhibited limitations, including low sensitivity, limited memory, resulting in significant variations in acquisition rates, limited processing capacity, requiring external post-processing hardware, and the need for an external vibration source not integrated into the monitoring system (typically an air fan) [25].

To address the challenges of the cost-effective system and the limitations of using ambient noise for excitation, which can have a low signal-to-noise ratio and be contaminated by existing ambient vibrations at certain frequencies [27], the research group developed two strategies to produce higher quality signal responses that are less susceptible to noise errors:

1. **Sine Sweep Excitation System**: A low-cost sine sweep excitation system was developed and tested on mortar specimens, producing high-quality signals with improved signal-to-noise ratios [25]. However, the system requires precise and complex control of the excitation signal, making it difficult to deploy.
2. **Impulse Excitation System**: This study focuses on developing a low-cost system based on impulse excitation. Impulse loads are a common technique in modal analysis [28,29] and involve applying a controlled, short-duration force (an impulse) to the specimen, producing a clear and distinct response with a high signal-to-noise ratio [28,30]. Impulse loads are mathematically white excitations in the frequency domain, possessing equal energy across all frequencies, and do not require monitoring of the load input [31]. These methods can be easily implemented using an ON-OFF switch and a solenoid, adding no complexity to the hardware and making the method cheaper and easier to deploy [28].

The primary objective of this study is to develop and present a low-cost system based on impulse excitation applied to a composite beam, introducing a new method for measuring the early elastic modulus of cementitious materials, referred to as EMM-IRM (Elasticity Modulus Measurement through Impulse Response Method). This system integrates the advantages of the composite beam configuration, which enables the assessment of cementitious materials from their earliest stages, with the operational simplicity and improved signal-to-noise ratio characteristic of impulse excitation. By addressing limitations in existing methods, this approach offers a practical alternative for the early-age characterization of cement pastes, balancing cost, simplicity, and measurement reliability. Despite its advantages, concerns arise regarding potential damage to the material during the early stages of mechanical property development. This study assesses the system's effectiveness in measuring the elastic modulus accurately throughout the fluid-to-solid phase transition. To validate the robustness and accuracy of the EMM-IRM system, tests were performed on Portland cement paste, with results compared against three established methods: conventional EMM-ARM, cyclic compression, and traditional impulse excitation techniques.

2. Methodology

2.1. Proposed system

The proposed setup consists of three parts: (i) the physical setup, comprised by the mould, support and lids; (ii) the hardware, comprised by the electronic components responsible for the excitation, acceleration acquisition and data analysis, and (iii) the software.

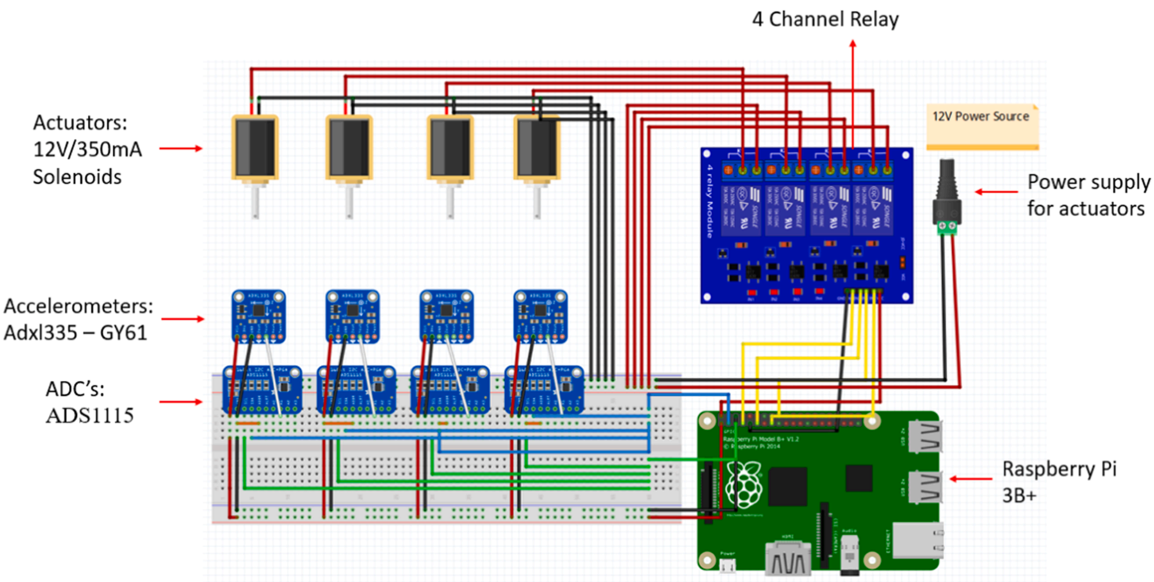

Fig. 2. Scheme of the Hardware.

2.1.1. Physical setup

A scheme of the proposed physical setup is presented in Fig. 1. The test setup, which was based on previous developments by [2,4,12,14,25,26], includes a PVC cantilever tube with internal and external diameters of $Ø_i$=16.75 mm and $Ø_e$=20 mm, respectively, inside of which the paste will be filled. This tube serves as the basic component of the system. In previous works [2,4,12,14,25,26], the cantilever tube was subjected to ambient forces (e.g., fan-generated wind) assumed as white noise on average and required a high slenderness ratio to be effectively vibrated. The main difference in the proposed setup is that the vibration of the beam is induced by an impulse from an actuator installed at the tip of the beam. With the actuator at the tip, controlled vibration at higher levels than ambient forces could be applied to the beam. Consequently, as experimentally evaluated, the slenderness ratio required for effective vibration of the cantilever beam could be reduced. Thus, the proposed system has a shorter free span length (350 mm) compared to previous versions (450 mm). Tests were conducted with specimens of shorter lengths, but satisfactory results could not be obtained. This is attributed to the capacitors present in the low-cost accelerometer used, which filter out frequencies above 50 Hz [32]. From Eq. (3), one can understand that as the sample length decreases, the natural frequency increases accordingly, leading to natural frequencies of specimens shorter than 350 mm exceeding 50 Hz. An attempt was made to find other low-cost accelerometers on the market with higher cut-off frequencies, but none were found.

2.1.2. Hardware

Unlike previous cement paste versions of EMM-ARM [2,4,12,14,26], the hardware presented in this work is not only responsible for collecting sample acceleration data, but it is also responsible for sample excitation and for processing the acceleration data obtained. As depicted in Fig. 2, a schematic of all system components is presented.

The hardware chosen is a cost-effective system that can have up to four different channels in a single, unified system to perform all tests in a fully automated manner with minimal user intervention. Subsequently, after positioning the samples in the proper position within the physical system, and initiating the system, it is able to excite the samples, collect the acceleration data, process the data, and present the modulus of elasticity data of the cementitious material in real-time to the user.

The 4-channel hardware is composed of:

(i) a Raspberry Pi 3 Model B+: The base component of the developed unified and integrated system is a Raspberry Pi Model 3B+. This choice was made due to its high performance and low cost. The Raspberry Pi 3 Model B+ is a single-board computer engineered for educational and industrial applications. Released in 2018, it features a 64-bit quad-core processor running at 1.4 GHz with 1 GB of RAM. Additionally, it has 4 USB 2.0 ports, wireless connectivity, and a range of other features. The Raspberry Pi Model 3B+ is equipped with 40 General Purpose Input/Output (GPIO) pins. These pins can be used to interface with other components in the circuit and control them. The GPIO pins can be used to read and write data to and from other devices, such as sensors, motors, and relays [33];

(ii) four ADXL335-GY61 accelerometers: The ADXL335 accelerometer [34] is the same used by Ribeiro et al. [26], which was identified as the most suitable sensor for this use based on a comparative performance study with six different accelerometers [35]. This accelerometer is a low-cost, low-power, 3-axis accelerometer and is utilized to measure the static acceleration of gravity or the dynamic acceleration due to motion, shock, or vibration. To facilitate the deployment of the ADXL335 into the project, a GY-61 breakout board [32] was used. This board integrates the ADXL335 sensor with the necessary circuitry to enable direct interfacing with the microcontroller board, such as a 3.3V-6V voltage regulator and 0.1 μF low-pass filter capacitors in each of the accelerometer axis data lines, leading to a bandwidth of 0.5 Hz to 50 Hz. This bandwidth is sufficient for the frequencies expected during the EMM-IRM test with cement pastes, which ranged between 20 Hz and 50 Hz with the test setup employed in this work;

(iii) four 16-bit Analog-to-Digital Converter (ADC) modules of the ADS1115 model: The ADS1115 ADC [36] modules play a crucial role in converting the analog output signals from the accelerometers into digital values that can be processed by the Raspberry Pi. With their high resolution of 16 bits, they ensure accurate and precise measurement of the accelerometer data [26];

(iv) four push-pull 12 V/1 A solenoids as the excitation actuators and their 12 V power supply: The four push-pull solenoids serve as excitation actuators in the hardware setup. They are responsible for generating controlled vibrations or mechanical movements based on the input signals received from the Raspberry Pi. The solenoids require a 12 V power supply to operate effectively;

Table 1
List of the main components of the proposed hardware and their respective prices.

Category	Component	Price (US$)
Fixed components	Raspberry Pi 3 - Model B+	35
	12 V Power Supply	1.5
	Breadboard	4.5
	Jumper Wires	3.95
Components that increase along with channel numbers.	ADXL335	14.95
	ADS1115	14.95
	Push-Pull Solenoid - 12VDC	7.5
	5 V Relay	1.5

(v) a 4-channel 5 V relay: The 4-channel relay acts as an interface between the Raspberry Pi and the solenoids. It allows the Raspberry Pi to control the activation and deactivation of each solenoid independently. The relay provides a reliable switching mechanism to ensure the proper timing and coordination of the solenoid operations in the 4-channel setup.

Table 1 provides a list of the main components of the proposed system along with their respective prices. The total cost of the proposed EMM-IRM system for applications involving two specimens is estimated at US$122.75 (EUR 114.28). This price is approximately one-fortieth of the cost of traditional systems (EUR 5000), which utilize professional structural monitoring accelerometers and commercial data acquisition systems, excluding software license costs [25]. Additionally, it is less than half the cost of the system proposed by Russo et al. (EUR 260), which is a cost-effective controlled excitation-based system [25].

2.1.3. *Impulse excitation source*

The physical principle of the proposed technique is based on traditional modal analysis techniques with impulse excitation, differing by being applied to a composite beam. Details about this methodology can be found in [28], [29] and [37]. As mentioned in the previous section, a 12 V/1 A push-pull solenoid was used to create the impulse excitation for the system developed in this work. Detailed information about this solenoid is presented in Fig. 1. Fig. 1(e) shows the dimensions of the solenoid used, and Fig. 1(f) displays its installation in the system. As depicted in Fig. 1(f), the solenoid is positioned and fixed just above the tip of the cantilever beam with a small gap between them. The solenoid is connected to a relay, which serves as an ON-OFF switch, and it is controlled by the Raspberry Pi. When the Raspberry Pi issues the command to open the switch, the rod in the middle of the solenoid descends and makes contact with the sample. When the switch is closed, the spring in the solenoid returns the rod to its initial position. Within a very short time interval, an impulse-type force is applied to the sample. The software developed for this work, as discussed in Section 2.1.3.1, is programmed to open and close the switch at 0.02-second intervals. This was the shortest timing observed experimentally for which the solenoid could effectively excite the beam. With this timing, the 12 V/1 A solenoid generates an impulse force, averaging approximately 0.19 N, inducing vibrations in the beam. This value was determined through tests involving the application of force using the same solenoid and time interval on a cantilever rectangular cross-section metallic bar with known properties ($L = 460$ mm, $EI = 23821269$ MPa mm^4, $x = 400$ mm, where L is the bar's length, and E and I are the modulus of elasticity and moment of inertia of the bar, respectively, and x is the distance from the fixed support where the LVDT (Linear Variable Differential Transformer) is placed). Force measurements were obtained by measuring deflection using an LVDT and applying Eq. (1), which is based on the Euler-Bernoulli beam theory [38](Fig. 3):

$$F = \frac{6EI\delta_x}{x^2(3L - x)} \tag{1}$$

In this equation, F is the static equivalent force of the solenoid, and δ_x is the deflection at distance x from the fixed support. These tests were conducted 20 times, resulting in an average maximum deflection of 0.21 mm and a corresponding equivalent static force of 0.19 N, with a standard deviation of 0.06. Additionally, tests were conducted at various distances in the range of 2 mm to 8 mm to assess their impact on the generated force. It was observed that the differences were negligible, and the solenoid can be installed and fixed above the tip of the specimen within the mentioned range of distances.

By obtaining the equivalent static force applied by the solenoid, it is possible to calculate the maximum bending moment in the cantilever beam and subsequently determine the maximum tensile stress using Eq. (2) derived from the Euler-Bernoulli beam theory [38]:

$$\sigma = \frac{M \bullet y}{I} \tag{2}$$

where σ is the bending stress, M is the maximum bending moment in the beam, y is the distance from the neutral axis to the point of interest, and I is the moment of inertia of the beam's cross-section. In the case of the composite beam presented in section 2.1.1, with a span length of 350 mm and a circular cross-section of 20 mm in diameter, the calculated maximum tensile stress applied by the solenoid is approximately 0.085 MPa.

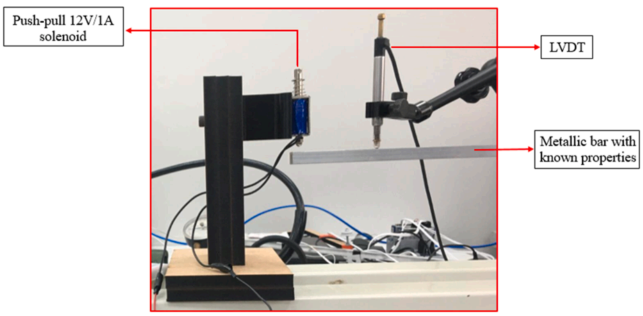

Fig. 3. Solenoid's applied force determination.

2.1.4. Procedure and Software

As presented in previous works [2,4,12,14,26], the EMM-ARM procedure involves conducting a test on a composite tube filled with a material of interest, obtaining the natural frequency of this composite tube, and calculating the elastic modulus of the internal material. Fig. 4 illustrates the step-by-step flowchart of the testing procedure for this work.

As depicted in the flowchart, the initial step of the testing procedure involves preparing all components of the physical system configuration. These components include PVC pipes cut to the appropriate size, lids, adhesive, and tape for securing the closing lids and accelerometer to the pipe. Subsequently, it is necessary to measure the total length of the pipes, as well as the mass applied at the tip of the beam, which encompasses the sum of the plastic lid masses, double-sided tape, adhesive, accelerometer, and a portion of the connected wires. To achieve this mass at the tip (M_t [g]), the accelerometer with three male-to-female jumper wires of 10 cm attached to it is affixed to one of the plastic lids using a piece of double-sided tape. The adhesive used to attach the plastic lid to the PVC pipe is applied around the lid, and this assembly is weighed just before being adhered to the PVC pipe. Once this measurement is obtained, the lid and accelerometer assembly are glued to one end of the PVC pipe, sealing that end. Next, the following step is to mix the material and record the time at which water first comes into contact with the cement. This will serve as the initial time (t_0), and all measurements of the elastic modulus obtained during the test are recorded relative to this time. Subsequently, the tube is filled with the cement paste using a funnel. To ensure there are no voids in the tube, vibration is applied along the length of the tube for a duration of 1 minute to eliminate any air bubbles within the tube. This vibration can take the form of lateral taps on the tube using a spatula. Once the tube is completely filled along its length, the other end of the tube is sealed with a plastic lid and adhesive tape, and the tube is weighed. By subtracting the mass of the components placed at the ends of the tube from this mass, the total mass of the full tube is determined (M_f [g]). Once this is obtained, the testing can commence. To do so, it is necessary to position the tube in the correct location, connect the accelerometer cables to the system, open the developed software, input the measurements, and initiate the software. This software, which will be discussed in more detail in the next section, is capable of calculating, saving, and plotting the modulus of elasticity of the internal material of the tube over the duration of the test. Fig. 1(f) depicts an actual image of the test and the developed EMM-IRM system.

2.1.4.1. Software.
The software developed for this system is written in the Python language, which is known for its user-friendly nature. Its design aims to provide a seamless and intuitive user experience. Fig. 5 illustrates the step-by-step algorithm that the software follows to determine the modulus of elasticity for the tested material.

Once the software is initiated, the first task it performs is to read the data that has been entered by the user. This includes the number of channels, which can range from 1 to 4, the duration of each acquisition package (d [s]), the interval duration between each package (di [s]), the total duration of the trial (D [days]), the internal diameter of the tube ($\O_i$ [mm]), the total length of the beam (L_t [mm]), the free span length of the beam (L [mm]), the mass at the tip of the beam (M_t [g]), the time that passed from t_0 (t [s]) and the total mass of the full tube (M_f [g]). Once the data has been read, the software then commands the solenoid to be turned on and off at an interval of 0.02 s. At this level, the software reads the acceleration of the beam which is captured by the accelerometer and the ADC with an acquisition frequency of 860 Hz, and saves it in a vector instantaneously. This frequency is the maximum acquisition frequency reported on the datasheet of the ADS1115 ADC [36], and was selected for a higher accuracy. Afterwards, this vector of accelerometers is stored in a separate TXT file along with the acquisition start time for future access. Subsequently, the software automatically opens all saved accelerometer TXT files and performs the following processes for each file. It first calculates the Power Spectrum Density (PSD) of the accelerometers using the Welch procedure [39]. Then, by analyzing the PSD, it identifies the first natural frequency of the beam, denoted as f [Hz], using the Peak-picking method. At this stage, the software calculates the EI of the composite tube (where E [GPa] is the elastic modulus of the composite tube and I [m^4] is its moment of inertia) from the natural frequency and appends it to a vector. Finally, it saves this information in a TXT file along with its respective acquisition time. This calculation is performed using Eq. (3), a simplified equation for the vibration frequency of a cantilever beam with a concentrated mass at its tip, as presented by [28].

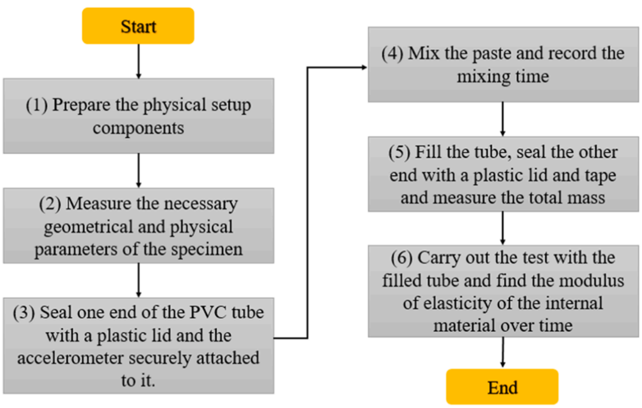

Fig. 4. Test procedure flowchart.

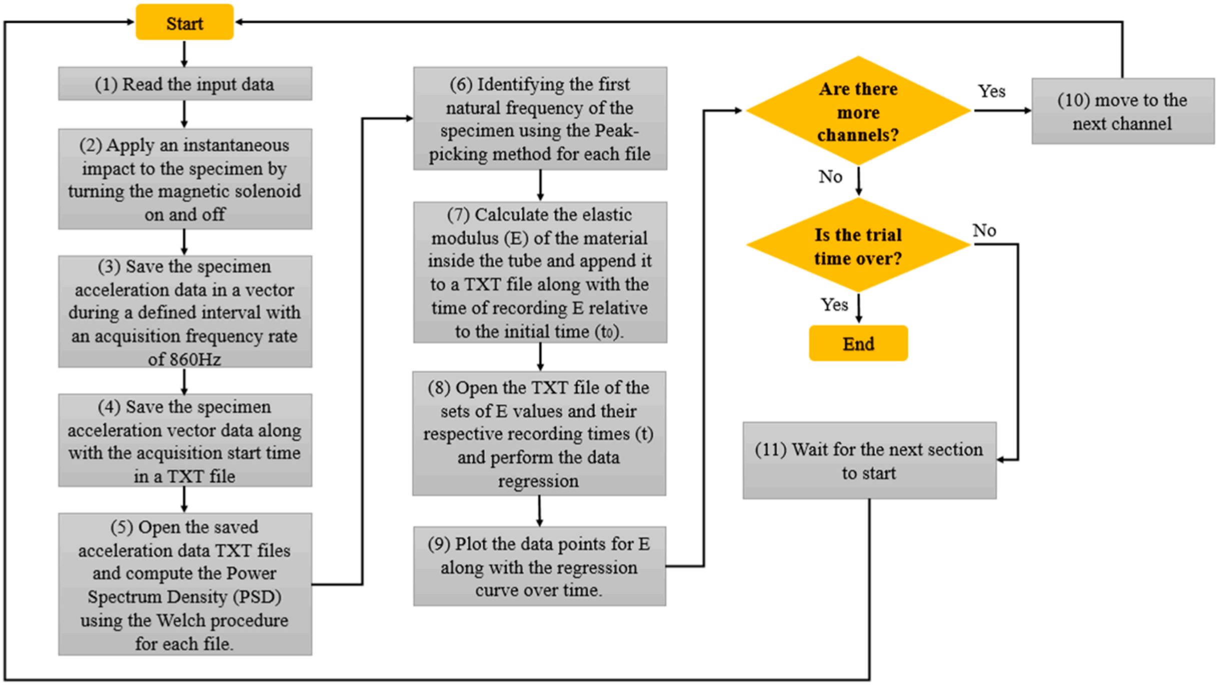

Fig. 5. Software algorithm.

$$EI = \frac{4}{3}\pi^2 f^2 L^3 M \tag{3}$$

In which M is the total equivalent mass at the free end of the full cantilever beam and is calculated through Eq. (4) [40]:

$$M = M_t + \frac{33}{140}\frac{M_f \times L}{L_t} \tag{4}$$

The next step is for the software to open the EI TXT file and calculate the elastic modulus of the cement paste inside the tube. In this phase, the first step is for the software to determine the E_eI_e of the empty tube (in which E_e [GPa] is the elastic modulus of the empty tube and I_e [m^4] is its moment of inertia). Based on previous EMM-ARM works [2,4,12,14,26] we have the relationship from Eq. (5):

$$EI = E_eI_e + E_cI_c \tag{5}$$

Where E_c [GPa] is the elastic modulus of the cement paste inside the tube and I_c [m^4] is its moment of inertia. As this test is conducted from early ages, and it is assumed that the cement paste inside the tube does not exhibit stiffness in the initial phase of the test, the software considers that E_c from the first recorded data of the test, and consequently E_cI_c is equal to zero. With this consideration, the software assumes that the value of E_eI_e to be used for calculating the progression of the elastic modulus of the cement paste is equal to the first EI value calculated by Eq1 and saved in the EI TXT file. Thus, the software will go straight ahead and calculate the elastic modulus of the paste within the tube and save it in a TXT file along with the time of registering the modulus. The calculation of the elastic modulus of the cement paste is done through Eq. (6):

$$E_c = \frac{EI - E_eI_e}{I_c} \tag{6}$$

Where I_c is the moment of inertia of the circular section of the cement paste inside the tube calculated by Eq. (7):

$$I_c = \frac{\pi}{64}\O_i^{\,4} \tag{7}$$

Subsequently, the software automatically opens the file containing the elasticity modulus values along with their corresponding timestamps. To obtain the elasticity modulus curve over time (E_t), the software performs a regression on the values stored in this file using Eq. (8).

$$E_t = a_1 \times e^{-\left(\frac{\tau_1}{t}\right)^{\beta_1}} + a_2 \times e^{-\left(\frac{\tau_2}{t}\right)^{\beta_2}} \tag{8}$$

Where a_1, a_2, τ_1, τ_2, β_1, and β_2 are parameters to be fitted. Eq. (8) is a two-component model based on a commonly used three-parameter model that describes the hydration kinetics of cementitious materials [41–45]. In the three-parameter model, a

represents the corresponding apparent ultimate value, while τ and β control the intercept and curvature of the plot on a logarithmic scale [41]. The use of two components, instead of the single component typically employed [41,44], improves the representation of early ages, significantly enhancing the smoothness of the elastic modulus estimates during these periods. At the same time, it ensures the fitting process remains solvable, as the inclusion of additional components often leads to convergence problems [46].

Finally, the software plots the data points for E_c and the regression curve over time and then moves on to the next channel or waits for the next section until the desired testing time is completed. All the code written for this software will be publicly shared on the platform GitHub through the link available in [47], after the publication of this article.

2.2. Validation

2.2.1. Materials and mixture proportions

A CP V-ARI, a high early strength Portland cement standardized in Brazil by NBR 16697 [48], was utilized to produce all the cement pastes used in the analysis. This cement, obtained from a single 50 kg bag, exhibits a characteristic compressive strengths of 16.4 MPa at 1 day and 40 MPa at 28 days, as determined by compressive resistance tests conducted in accordance with the Brazilian standard NBR 7215 [49].

The cement pastes were prepared with a water-to-cement ratio of 0.5. The mixing procedure for the cement paste followed the guidelines outlined in NBR NM 43 [50], which consisted of the following steps: (i) Pour the water into the mixing bowl; (ii) Gradually add all the cement (t_0) and wait for 30 seconds; (iii) Mix at a low speed with a paddle rotation of 140 ± 5 r/min and a planetary rotation of 62 ± 5 r/min for 30 seconds; (iv) Cease mixing, scrape the sides of the bowl for 30 seconds, and wait an additional 30 seconds; (v) Resume mixing at a high speed with a paddle rotation of 285 ± 10 r/min and a planetary rotation of 125 ± 10 r/min for 60 seconds.

2.2.2. Conducted experiments

As outlined in the introduction, there are concerns about potential damage to the material being tested due to the impulse applied to the specimen, particularly during the fluid-to-solid transition phase. Such damage could result in permanent changes to the material's mechanical properties, including the modulus of elasticity. To address this issue, the system described in section ↱2.1 was developed with precautions aimed at maintaining low applied stress levels.

Key design considerations for the system included the selection of a cost-effective solenoid capable of applying minimal loads, the reduction of the free span length to decrease material stress, and the optimization of force application duration (ON-OFF switch timing) to ensure effective operation without excessive force. The distance from the solenoid to the specimen was also assessed, revealing only a minimal effect on the resultant force. As a result, the developed system applies a maximum tensile stress of approximately 0.085 MPa to the composite beam (as detailed in section ↱2.1.2.1).

It is important to emphasize that this applied stress does not uniformly affect the internal material. The 0.085 MPa value represents the approximate maximum stress on the composite beam, while the actual stress experienced by the material inside the mold can be significantly lower, especially during the initial phases when the material lacks strength. Since the material is housed within a tube and is assumed to function in a composite manner, both the internal material and the mold experience the same displacement during vibration. Due to the greater stiffness of the mold, it absorbs more force and, consequently, more stress. Initially, the material within the mold exhibits minimal stiffness, causing most of the applied stress to be absorbed by the mold. As the cement paste gains strength over time, it begins to take on a larger proportion of the applied stress.

To assess the magnitude of the maximum stress applied by the solenoid to the composite beam, it can be compared with the estimated tensile strength of the cement paste used in this study, as detailed in the previous section. The average tensile strength (f_{ctm}) of this material can be estimated using Eq. (9) [51,52], based on the characteristic compressive strength (f_{ck}) of the material:

$$f_{ctm} = 0.3 \quad f_{ck}^{2/3} \tag{9}$$

The cement paste exhibited compressive strengths of 3.88 MPa at 1 day and 10.48 MPa at 3 days, obtained from cyclic compression tests, allowing for the estimation of average tensile strengths of 0.74 MPa and 1.44 MPa for days 1 and 3, respectively. This indicates that the tensile stress applied by the solenoid is significantly lower than the material's tensile strength, even at just 1 day of age. Consequently, the 1-day-old material, even without the mold, can withstand the stress applied by the solenoid without damage.

During the initial stages, when the material remains in a liquid state (prior to setting), there are minimal concerns regarding damage. Although the applied stress is very low, uncertainties remain regarding the fluid-to-solid transition phase. This phase complicates the assessment of applied stress and tensile resistance, making it challenging to determine whether any damage occurs that could affect the evolution of the material's mechanical properties. Current literature lacks the necessary evaluations or experimental results to establish maximum force application limits during the fluid-to-solid transition to prevent damage; therefore, this assessment must be conducted experimentally.

To evaluate the effectiveness of the developed EMM-IRM system and its influence on the mechanical properties of the material, a practical assessment can be conducted using the system itself. This involves utilizing two test specimens constructed with a mold filled with cementitious material. One specimen is allowed to rest until the material inside the mold achieves a tensile strength considerably greater than the stress applied by the solenoid. Simultaneously, the second specimen is subjected to impulse excitation immediately after mixing the cement with water. Once the resting specimen attains a strength above the solenoid's applied stress, it is tested to determine its modulus of elasticity using the same EMM-IRM system. If the modulus of elasticity obtained from the impulse-excited specimen closely matches that of the resting specimen at the same age, it suggests that the applied impulse has not caused any damage to the material during its early stages of development.

Before proceeding with validation of the developed EMM-IRM system against well-established methods, this verification was conducted using two specimens filled with the material presented in section 2.2.1. The modulus of elasticity for both specimens at 7 days of age exhibited very close values, with a difference of only 0.52 %, which is inherent to sample variability. This result is a positive indication that the developed system does not damage the tested material.

For validation of the newly developed system against other well-established methods, a series of tests were performed using both

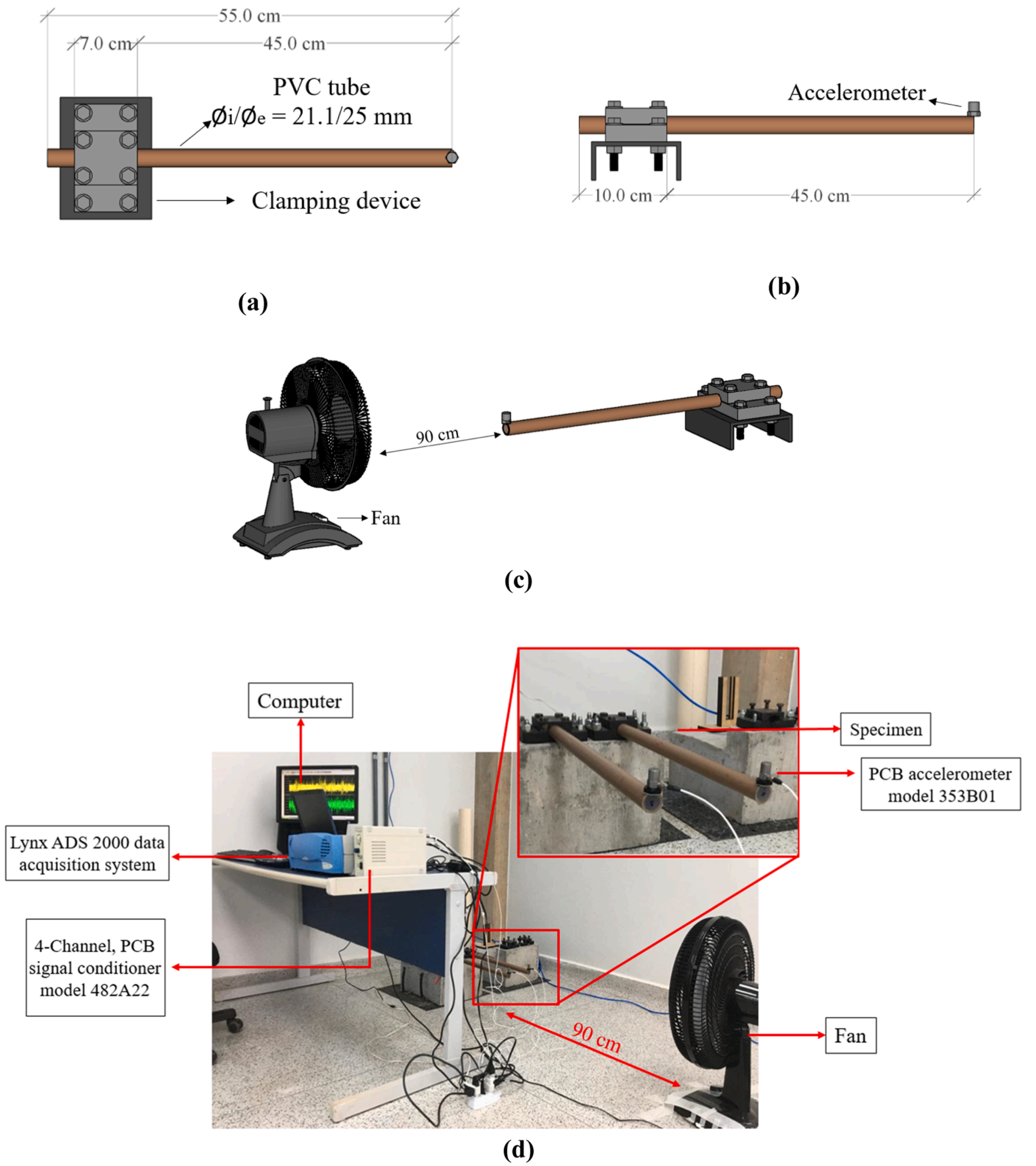

Fig. 6. Scheme of the conventional EMM-ARM setup: **(a)** Top view of the test systems; **(b)** Front view of the test systems; **(c)** Relative position between test systems and fan; **(d)** Conducted EMM-ARM test.

the new system and three alternative methods: cyclic compression, the traditional impulse excitation technique, and the conventional EMM-ARM setup. A comparative analysis of the results was subsequently conducted. The technique chosen to validate the EMM-IRM at very early ages (up to 1 day old) was the conventional EMM-ARM technique, which has been widely validated for this phase of the fluid-to-solid transition compared to other standard methods [12]. In addition to the conventional EMM-ARM technique, cyclic compression and traditional impulse excitation techniques, which require demolding of the specimen, were used to reinforce the validation at more advanced stages. This study focused on validating the technique for determining the modulus of elasticity of cement paste up to 7 days old. Tests using cyclic compression and the traditional impulse excitation technique were planned for 1, 3, and 7 days; however, due to technical issues with the testing equipment, data for cyclic compression were only available for 1 and 3 days.

The testing procedure of the proposed system followed the identical steps as elucidated in section ↱2.1.3. This encompassed the utilization of 5-second duration packages with a 10-minute time interval between each package, consistently maintained for a period of 7 consecutive days. The other experiments conducted, along with their respective procedures aimed at validating the newly developed system, will be detailed in the subsequent sections.

2.2.2.1. Cyclic Compression. The cyclic compression tests were conducted on three cylindrical specimens with a diameter of 5 cm and a height of 10 cm, at ages of one and three days. Prior to the tests, the compressive strength was determined using three additional specimens for each age. To ensure proper curing, all specimens were enveloped in plastic film and submerged in a water-filled bucket. The measurement test for the elastic modulus (E-modulus) followed a specific protocol, adhering to the guidelines outlined in the Brazilian standard ABNT NBR 8522 [53], which closely resembles the ASTM C469 [54] procedure. The procedure entailed the following steps: (i) Initiate the elastic modulus measurement by subjecting the specimen to a stress level equivalent to 30 % of its compressive strength, maintaining it for a duration of 60 seconds; (ii) Subsequently, decrease the applied stress to 0.5 MPa and sustain it for an additional 60 seconds; (iii) Repeat steps (i) and (ii) consecutively; (iv) During the second repetition, record the strain after 30 seconds of applying the 0.5 MPa stress; (v) Apply a stress level equivalent to 30 % of the compressive strength, record the strain after 30 seconds, and sustain it for 60 seconds. The strain was calculated averaging the values calculated based on the readings of two displacement transducers positioned in opposite sides of the specimen and with reference length equal to 5 cm. The load was registered using a load cell.

2.2.2.2. Traditional Impulse Excitation Technique (TIET). The traditional impulse excitation technique entails stimulating the demolded specimen through the application of a single impact and capturing the corresponding acoustic response using an acoustic sensor. The fundamental flexional frequency of vibration, and consequently the dynamic modulus of elasticity, is determined by analyzing the acoustic response. This analysis involves the utilization of digital signal processing methods or counting zero crossings within the recorded waveform. The ASTM C215–19 [55] standard outlines the primary methodologies for characterizing the dynamic elastic moduli of concrete specimens, including the impact excitation technique. In this study, a Sonelastic System [56] for cementitious materials was employed, which automates all the aforementioned processes and adheres to the ASTM C215–19 [55] standard test method. Five test specimens with diameters ranging from 16.55 to 16.64 mm and heights between 70.23 and 73.36 mm were examined using the Sonelastic system at ages of one, three, and seven days. After demoulding on the first day, all specimens were wrapped in plastic film and cured in water.

2.2.2.3. Conventional EMM-ARM. The conventional EMM-ARM test in this context refers to a test setup in which a fan is used to generate an ambient vibration of the white noise type on a composite slender beam filled with the material of interest and this vibration is registered using structural monitoring accelerometers and acquisition systems. Fig. 6 displays a schematic of the physical setup used for this work. The embedded beam of this setup is the same one used in Ribeiro's work [26], which is a PVC pipe with an outer diameter of $Ø_e$=25 mm, inner diameter of $Ø_i$=21.1 mm and a free span length of 450 mm. A 30 cm diameter fan with an average airflow of 0.680 m^3/s, 44.86 W of power, and a rotation speed ranging from 1200 to 1500 rpm was used to enhance the ambient vibration. The relative positioning between the fan and the testing systems remained constant throughout the experiment.

Two specimens were tested using this setup, in which to detect the vibrations in the samples, a Lynx ADS 2000 data acquisition system [57] was used in conjunction with professional PCB accelerometers, model 353B01. These accelerometers are of the general purpose, quartz shear ICP type, with a sensitivity of 20 mV/g, and a frequency range of 1–7 kHz [58]. Additionally, a 4-channel signal conditioner model 482A22 was employed in the setup [59]. The Lynx control software, known as AQ Dados7, was utilized for acquiring data from the accelerometers. The accelerometers were configured to record 60-second data packages at a frequency of 500 Hz, which is the same data acquisition setup employed by Granja in his study [3]. The acquisition of the accelerometers was conducted at regular intervals of 10 minutes over a period of one week. For the post-processing of the acceleration data and the calculation of the specimens' elastic modulus, the same software as described in section ↱2.1.3.1 was used, beginning from step 5 to

Table 2
Elastic modulus results from the Cyclic Compression tests.

Age [days]	Elastic modulus from the Cyclic Compression tests [GPa]				
	Specimen1	Specimen2	Specimen3	Average	Standard deviation
1.16	3.34	2.80	2.99	3.04	0.22
3.17	7.21	6.42	7.44	7.02	0.44

step 9, as displayed in Fig. 5. Fig. 6(d) depicts an actual image of the conducted EMM-ARM test.

3. Results and discussion

3.1. Cyclic Compression

The results of Cyclic Compression tests for the three specimens, along with the average values and standard deviation, are presented in Table 2.

3.2. Traditional impulse excitation technique

The results of traditional impulse excitation tests for the five specimens, along with the average values and standard deviation, are presented in Table 3. As mentioned earlier, the value of the elasticity modulus obtained through the traditional impulse excitation technique is the dynamic modulus of the material. Since there is no definitive relationship between the dynamic and static modulus [52], only the kinetics of the normalized values from this method and the developed EMM-IRM method will be compared in this study.

3.3. Conventional EMM-ARM

The results of the conventional EMM-ARM test for the two specimens are presented in Fig. 7. The graph in Fig. 7(a) represents the evolution of the elastic modulus for both specimens over time, with each data point corresponding to an estimated elastic modulus obtained from a measurement session. A clear and consistent superposition of the curves obtained for both specimens can be observed in this graph. The average standard deviation of the measurements for both specimens throughout the entire duration of the experiment was calculated as 0.08.

Fig. 7(b) displays the regression curve, derived using Eq. (8), encompassing all elastic modulus data points obtained for each specimen during the entire test. The corresponding fitting parameters for each sample are listed in Table 4. Furthermore, Fig. 7(b) also displays the average curve, which will be instrumental in section ↱3.5 of this study, enabling a comprehensive comparison of the average results obtained from all static techniques employed in this research.

Finally, in order to compare the EMM-ARM data with the punctual data obtained from the tests of cyclic compression and traditional impulse excitation technique, the elastic modulus values for both samples were calculated using Eq. (8) and the fitting parameters presented in Table 4. These calculated values, along with their corresponding mean and standard deviation, are presented in Table 5. As depicted in Table 4, the fitting parameters derived from the regression analysis for specimens 1 and 2 in the conventional EMM-ARM exhibit distinct values. However, the coherence of these fitting curves with the experimental data is striking (refer to Fig. 7). Furthermore, upon scrutinizing Eq. (8), it becomes apparent that the asymptotic modulus of elasticity corresponds to the sum of parameters a_1 and a_2 for an infinite time span. According to the results in Table 4, the sum of these parameters results in 11.88 and 11.23 for specimens 1 and 2, respectively, which present very close values at infinite time.

3.4. Proposed EMM-IRM system

Similar to the previous section, Fig. 8 presents the results obtained from tests using the newly developed EMM-IRM system, where Fig. 8(a) illustrates the evolution of the elastic modulus for both specimens over time, and Fig. 8(b) depicts the regression curve of these data points using Eq. (8). Just like the conventional system, a clear and consistent superposition of the curves obtained for both samples can be observed in these graphs. The average standard deviation of the measurements for both specimens throughout the entire duration of the experiment was calculated as 0.06. This indicates that the newly developed system demonstrates good repeatability performance.

In Table 4 is presented the corresponding fitting parameters obtained for the curves presented in Fig. 8(b), while Table 5 provides the values of elastic modulus for both samples at ages one, three, and seven days, extracted from these curves.

3.5. Comparison of the proposed system to other static techniques

In Fig. 9, the average results of the elastic modulus from the three conducted tests with static elastic modulus results are presented. These tests include Cyclic Compression, the conventional EMM-ARM, and the proposed EMM-IRM tests. To offer a more distinct visualization of the ranges of variations, the graph not only includes the average data but also depicts the data variation intervals,

Table 3
Elastic modulus results from the Traditional Impulse Excitation tests.

Age [days]	Dynamic elastic modulus from the Traditional Impulse Excitation tests [GPa]						
	Specimen1	Specimen2	Specimen3	Specimen4	Specimen5	Average	Standard deviation
1.16	3.82	4.06	3.93	3.81	4.3	3.98	0.18
3.17	10.25	9.89	10.2	9.73	10.45	10.1	0.26
7.25	13.36	13.02	13.39	12.88	13.54	13.24	0.25

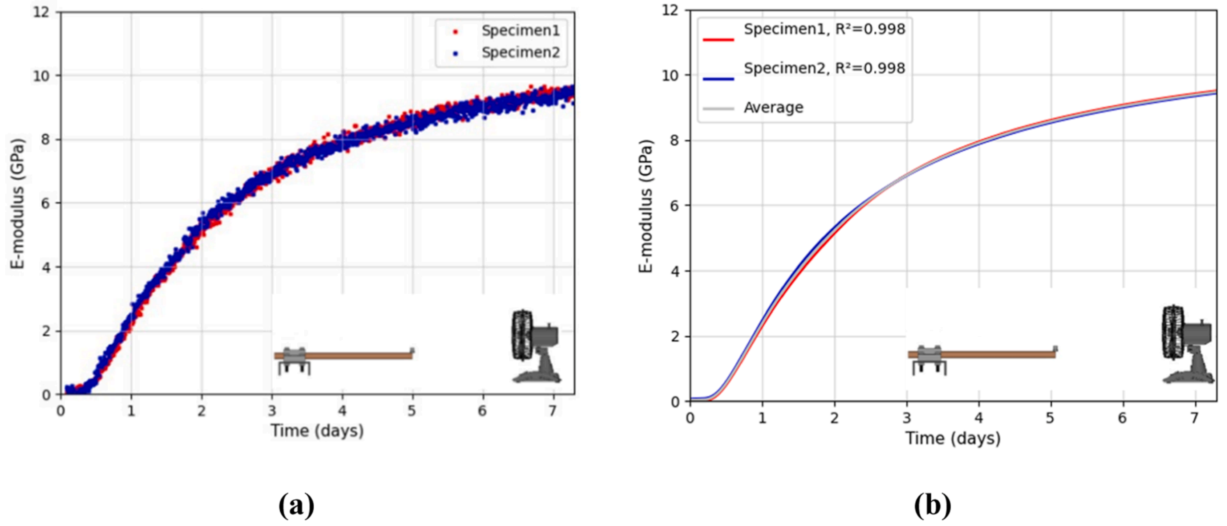

Fig. 7. Conventional EMM-ARM results: **(a)** E-modulus estimates; **(b)** Regression curves.

Table 4
The fitting parameters obtained from the regression curves.

Fitted parameters	Conventional EMM-ARM test		EMM-IRM test	
	Specimen1	Specimen2	Specimen1	Specimen2
a_1	0.413	9.12	4.28	5.41
τ_1	53.636	47.9	74.37	68.09
β_1	4.39	1.17	1.58	1.54
a_2	11.474	2.11	6.64	5.46
τ_2	39.177	13.97	24.86	21.87
β_2	0.973	1.9	1.35	1.57

Table 5
Elastic modulus results from the Conventional EMM-ARM and the proposed EMM-IRM tests [GPa].

Age (days)	Conventional EMM-ARM test				Proposed EMM-IRM test			
	Specimen1	Specimen2	Average	Standard deviation	Specimen1	Specimen2	Average	Standard deviation
0.6	0.812	0.878	0.845	0.033	0.817	0.796	0.807	0.011
0.8	1.550	1.721	1.635	0.085	1.607	1.606	1.606	0.000
1.16	2.840	2.992	2.916	0.076	2.847	2.846	2.847	0.001
3.17	7.127	7.115	7.121	0.006	6.955	7.067	7.011	0.056
7.25	9.488	9.391	9.440	0.049	9.471	9.527	9.499	0.028

represented as one standard deviation above and below the average values, for the Cyclic Compression data. This is due to the fact that the results of Cyclic Compression exhibited larger standard deviations compared to the results of EMM-ARM and EMM-IRM (Tables 1, 4, and 6). This graph provides a clear visual indication that the results obtained from the proposed system closely align with those from the other two methods.

For a better understanding of the data in Fig. 9, the average values of the elastic modulus from all static tests at different ages are presented together in Table 6. It is evident that all the tests exhibited very close values across all ages. Table 6 also presents the deviation of the average values of the elastic modulus obtained by the proposed EMM-IRM system compared to the other two methods at different ages. The average deviation of the EMM-IRM results in comparison to the other two methods at the three ages was found to be −2 %. It can be observed that the average results of the proposed system for the seven-day interval were slightly lower than the other methods, but not significantly so, and it should not be interpreted as sample damage due to the impulse. This observation can be supported by the fact that the data indicates the results of the proposed system are growing in conjunction with the other methods, and this error diminishes as the ages progress. The maximum deviation observed was in the comparison with the average value of the first day of the Cyclic Compression test, which amounted to 6 %. This difference can be explained by the fact that the comparison is made between average values, and since the Cyclic Compression test exhibited a larger range of variation, the error also increased.

Nevertheless, it is important to note that the proposed system presented values close to those of other static techniques and fell within the range of variation of the Cyclic Compression test, which indicates the validation of the system.

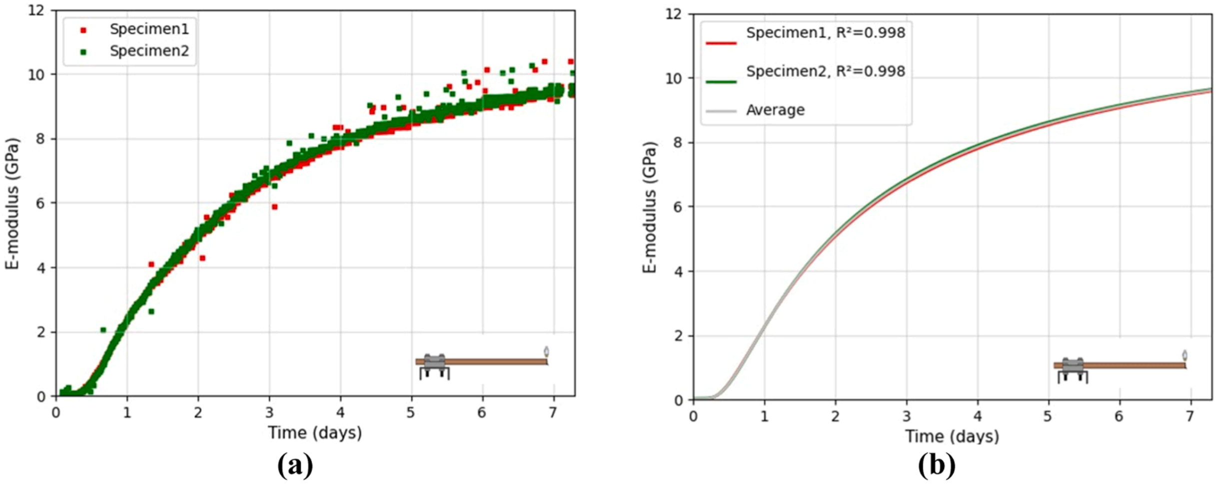

Fig. 8. Proposed EMM-IRM system results: (a) E-modulus estimates; (b) Regression curves.

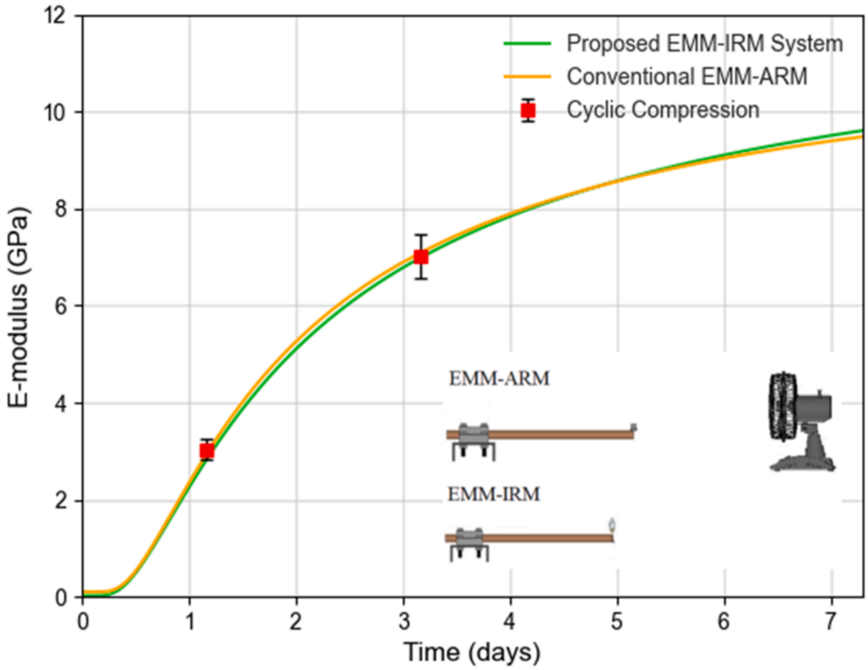

Fig. 9. Evolution curve of the average elastic modulus from the three static techniques: Cyclic Compression, conventional EMM-ARM, and proposed EMM-IRM tests.

Table 6
Comparison between the average elastic modulus values acquired from the proposed system and those originating from other static methods.

Age [days]	Test Method				
	EMM-IRM	EMM-ARM		Cyclic Compression	
	Elastic Modulus (GPa)	Elastic Modulus (GPa)	EMM-IRM Deviation (%)	Elastic Modulus (GPa)	EMM-IRM Deviation (%)
0.6	0.807	0.845	−4.50 %	-	-
0.8	1.606	1.635	−1.77 %	-	-
1.16	2.847	2.916	−2.34 %	3.040	−6.33 %
3.17	7.011	7.121	−1.54 %	7.020	−0.13 %
7.25	9.499	9.440	0.63 %	-	-

3.6. Comparison of the proposed system to the traditional impulse excitation technique

In cementitious materials, the ratio of the static modulus to the dynamic modulus is always smaller than unity and increases as the material's strength develops. This variable ratio prevents a straightforward conversion between the dynamic and static moduli [52]. In this section, the kinetics of the normalized static modulus values obtained by the proposed EMM-IRM system are compared with the dynamic modulus values obtained through the traditional impulse excitation technique.

The normalized static modulus obtained from the EMM-IRM system and the dynamic modulus from the impulse excitation technique, both normalized to their values at more advanced ages where the material exhibits greater strength, are expected to follow specific trends. Since the static-to-dynamic modulus ratio increases with material strength, the normalized dynamic modulus at earlier ages should ideally be higher than the corresponding normalized static modulus. If the opposite occurs, with the normalized static modulus exceeding the dynamic modulus, this could signal potential damage to the material, negatively affecting its mechanical properties. This would result in a greater difference between the static modulus measured by EMM-IRM and the dynamic modulus from the impulse excitation technique, leading to a lower static-to-dynamic modulus ratio at advanced ages, which is not typical for cementitious materials.

The average modulus results from both methods, normalized to their seven-day values, are presented in Fig. 10. The EMM-IRM system showed deviations of −0.20 %, −3.27 %, and 0 % at 1, 3, and 7 days, respectively, when compared to the traditional impulse excitation technique. The 0 % error at seven days is a result of normalization based on the seven-day measurements. These findings indicate typical behavior in the modulus curves obtained by EMM-IRM, consistent with the expected characteristics of cementitious materials, with no evidence of any damage to the specimens caused by impulse excitation.

3.7. Signal comparison (EMM-ARM VS EMM-IRM)

Fig. 11 illustrates the acceleration signals obtained from one of the test packages, conducted using both the conventional EMM-ARM system and the proposed EMM-IRM system at seven days of age, which are representative of the other specimens tested. These signals are presented in both the time domain (Fig. 11 (a)) and the frequency domain (Fig. 11 (b)). In the frequency domain, it is evident that the two systems exhibit distinct natural frequencies for their respective samples, despite being tested at the same age. This difference arises due to the varying sample lengths between the two tests. In the EMM-IRM system, the reduced sample length resulted in an increased natural vibration frequency.

Moreover, Fig. 11 (b) also reveals that the EMM-IRM system achieved a substantially higher signal-to-noise ratio compared to the conventional EMM-ARM system. It is important to note that these results compare signals from a professional accelerometer in the EMM-ARM system with those from a low-cost accelerometer in the EMM-IRM system. If the comparison were made against a low-cost EMM-ARM system using a similar low-cost sensor, the difference would likely be even more pronounced. Thus, despite being a low-cost solution, the EMM-IRM system, utilizing impulse excitation, significantly enhances signal quality and improves the accuracy of early-stage elastic modulus measurements. This approach overcomes the sensitivity limitations typically associated with low-cost EMM-ARM systems, which rely on ambient noise as an excitation source.

In environments characterized by high ambient noise contamination, such as construction sites or engineering laboratories where heavy machinery operates, the use of the EMM-IRM system is expected to be particularly advantageous. This is attributed to two primary factors. First, the EMM-IRM system provides an improved signal-to-noise ratio, which minimizes interference from environmental vibrations that may introduce peaks in the spectrum at frequencies unrelated to the natural frequency of the sample. A higher signal-to-noise ratio enhances the detection of the natural frequency, thereby reducing detection errors.

Second, the duration of the EMM-IRM test is significantly shorter than that of the EMM-ARM test. This reduction in testing time diminishes the potential impact of environmental noise contamination due to shorter exposure to such disturbances. This advantage is illustrated in Fig. 11 (a), which presents the signal obtained from the EMM-IRM system in the time domain. Fig. 12 provides a close-up view of the signal obtained by the EMM-IRM system in the time domain.

However, this study lacks experimental data from environments with high ambient noise contamination. To facilitate a more comprehensive comparison of the EMM-ARM and EMM-IRM systems in such settings, further experimental analyses are recommended. Future tests could involve three systems: the EMM-IRM, traditional EMM-ARM with professional, high-sensitivity accelerometers, and low-cost EMM-ARM systems with low-cost accelerometers.

4. Conclusion

This study developed a low-cost system based on impulse excitation applied to a composite beam, proposing a new method for measuring the early elastic modulus of cementitious materials, referred to as EMM-IRM (Elasticity Modulus Measurement through Impulse Response Method). Compared to EMM-ARM systems that rely on ambient noise excitation, the EMM-IRM method significantly reduces noise sensitivity, enhances signal quality, and improves the accuracy of early elastic modulus measurements. Additionally, it is easier to deploy than controlled excitation-based systems, which require complex signal control. The proposed system is approximately 40 times less expensive than traditional EMM-ARM systems (excluding software licenses) and costs less than half of low-cost controlled excitation-based systems, as it does not require additional excitation control components.

The viability of the proposed system was experimentally validated by comparing its results with those from three established methods: conventional EMM-ARM, cyclic compression, and traditional impulse excitation techniques. The analysis revealed a maximum variation of 6.33 % compared to these methods, confirming its reliable performance.

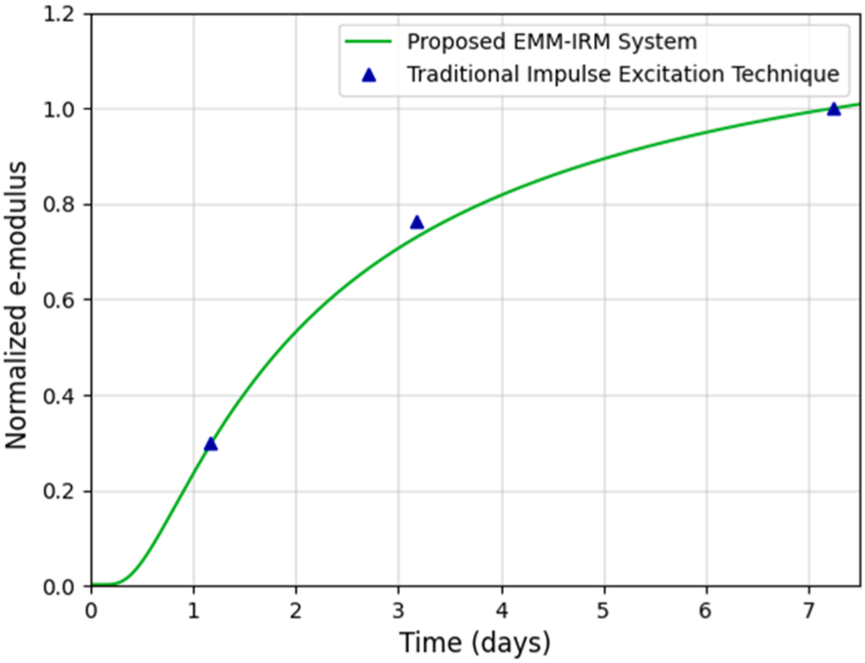

Fig. 10. Evolution curve of the normalized average elastic modulus from the EMM-IRM and the Traditional Impulse Excitation tests.

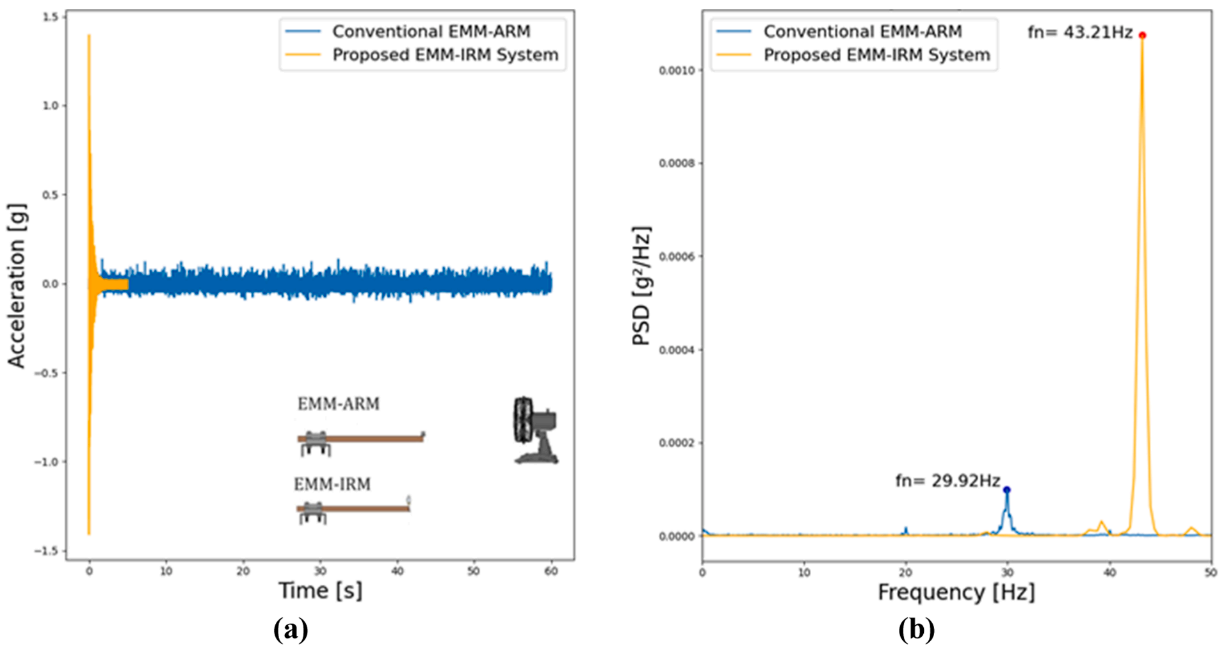

Fig. 11. Signals obtained from both conventional EMM-ARM tests and the proposed EMM-IRM system at 7 days of age: **(a)** Time domain; **(b)** Frequency domain.

The stress levels applied through impulse excitation in the proposed system were found to be very low, and validation against established methods indicated no significant damage to the tested materials that could adversely affect their mechanical properties. However, further investigations are required to evaluate the method's suitability across a broader range of materials and to assess any potential detrimental effects, particularly in the early phases when cement pastes exhibit reduced durability. It is advisable that, when applying this technique to new material types, well-established tests such as cyclic compression be conducted simultaneously, even at later ages, to compare the results for validation. If other testing methods are not available, the EMM-IRM system itself can be used to

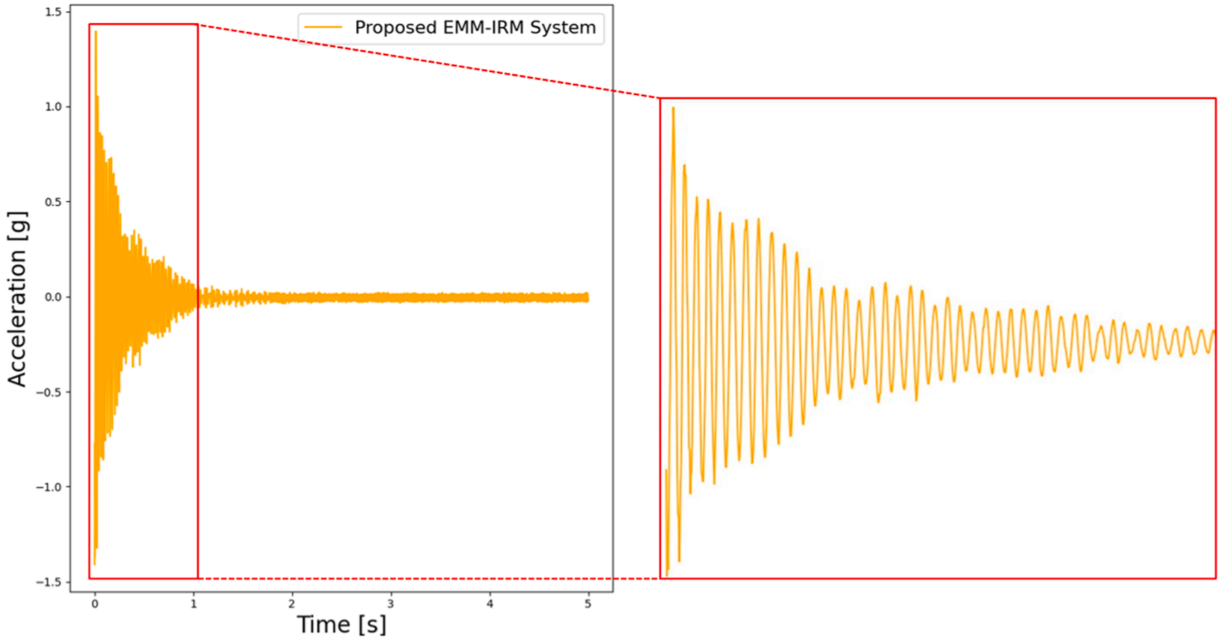

Fig. 12. Close-up view of the signal obtained from the proposed EMM-IRM system at 7 days of age.

determine whether the material has sustained any significant damage affecting its properties, as demonstrated in the validation section of this study.

Future work should explore the application of this technique to a range of materials, including different cement types, water-cement ratios, and various additives and composites. This will help determine whether adjustments to the applied force are necessary and establish limits for force and stress applicable to different material types or cement classes.

To encourage the widespread adoption of the proposed system, which provides a practical alternative for the early-age characterization of cementitious materials while balancing cost, simplicity, and measurement accuracy, the developed codes will be made publicly available on GitHub [47] following the release of this article. This will enable researchers and industry professionals to leverage the findings of this study.

CRediT authorship contribution statement

Renan Ribeiro: Writing – review & editing, Methodology, Conceptualization. **Thomas Russo:** Writing – review & editing. **José Granja:** Writing – review & editing. **Miguel Azenha:** Writing – review & editing, Conceptualization. **Rodrigo de Melo Lameiras:** Writing – review & editing, Supervision, Conceptualization. **Amir Araghi:** Writing – original draft, Software, Methodology, Investigation, Formal analysis, Conceptualization.

Declaration of Competing Interest

The authors declare that they have no known competing financial interests or personal relationships that could have appeared to influence the work reported in this paper.

Acknowledgments

This work was supported by the following Brazilian research agencies: CAPES, CNPq, and FAPDF. The first author is funded by grant number 142127/2020-5 from the Brazilian National Council for Scientific and Technological Development (CNPq). The second author is funded by grant number 153378/2022 from the Foundation for Science and Technology of Portugal (FCT). The second, third, fourth, and fifth authors were partly financed by FCT/MCTES through national funds (PIDDAC) under the R&D Unit Institute for Sustainability and Innovation in Structural Engineering (ISISE), under reference UIDB/04029/2020, and under the Associate Laboratory Advanced Production and Intelligent Systems ARISE under reference LA/P/0112/2020. This project has received funding from the European Union's Horizon 2020 under the Marie Sklodowska-Curie project SUBLime [Grant Agreement n. 955986].

Data Availability

Data will be made available on request.

References

[1] John V.M., editor. Report of UNEP SBCI WORKING GROUP ON LOW-CO2 ECO-EFFICIENT CEMENT-BASED MATERIALS. 2018.
[2] M. Azenha, F. Magalhães, R. Faria, Á. Cunha, Measurement of concrete E-modulus evolution since casting: A novel method based on ambient vibration, Cem. Concr. Res 40 (2010) 1096–1105, https://doi.org/10.1016/j.cemconres.2010.02.014.
[3] L. Maia, M. Azenha, M. Geiker, J. Figueiras, E-modulus evolution and its relation to solids formation of pastes from commercial cements, Cem. Concr. Res 42 (2012) 928–936, https://doi.org/10.1016/j.cemconres.2012.03.013.
[4] M. Azenha, R. Faria, F. Magalhães, L. Ramos, Á. Cunha, Measurement of the E-modulus of cement pastes and mortars since casting, using a vibration based technique, Mater. Struct. Constr. 45 (2012) 81–92, https://doi.org/10.1617/s11527-011-9750-9.
[5] L. Maia, H. Figueiras, S. Nunes, M. Azenha, J. Figueiras, Influence of shrinkage reducing admixtures on distinct SCC mix compositions, Constr. Build. Mater. 35 (2012) 304–312, https://doi.org/10.1016/j.conbuildmat.2012.02.033.
[6] M. Azenha, L.F. Ramos, R. Aguilar, J.L. Granja, Continuous monitoring of concrete E-modulus since casting based on modal identification: a case study for in situ application, Cem. Concr. Compos 34 (2012) 881–890, https://doi.org/10.1016/j.cemconcomp.2012.04.004.
[7] C. Boulay, E. Merliot, S. Staquet, O. Marzouk, Monitoring of the concrete setting with an automatic method, in: M.C. Forde (Ed.), Struct. Faults Repair - 2010, Engineering Technics press, Edinburgh, 2010, p. 11.
[8] J. Silva, M. Azenha, A.G. Correia, C. Ferreira, Continuous stiffness assessment of cement-stabilised soils from early age, Geotechnique 63 (2013) 1419–1432, https://doi.org/10.1680/geot.13.P.021.
[9] J. Silva, M. Azenha, A. Gomes Correia, J. Granja, Continuous monitoring of sand–cement stiffness starting from layer compaction with a resonant frequency-based method: Issues on mould geometry and sampling, Soils Found. 54 (2014) 56–66, https://doi.org/10.1016/j.sandf.2013.12.006.
[10] J.L. Granja, M. Azenha, C. De Sousa, C. Ferreira, Comparison between different experimental techniques for stiffness monitoring of cement pastes, J. Adv. Concr. Technol. 12 (2014) 46–61, https://doi.org/10.3151/jact.12.46.
[11] P. Fernandes, J. Granja, J. Sena-Cruz, M. Azenha, A. Benedetti, A new methodology for assisting quality control of NSM-CFRP systems since very early ages. 7th Int. Conf. FRP Compos. Civ. Eng., Vancouver, Canada, 2014.
[12] Granja J.L.D.. Continuous characterization of stiffness of cement based materials: experimental analysis and micro-mechanics modelling. University of Minho, 2016.
[13] M. Velay-Lizancos, M. Azenha, I. Martínez-Lage, P. Vázquez-Burgo, Addition of biomass ash in concrete: Effects on E-Modulus, electrical conductivity at early ages and their correlation, Constr. Build. Mater. 157 (2017) 1126–1132, https://doi.org/10.1016/j.conbuildmat.2017.09.179.
[14] J. Granja, M. Azenha, Elastic modulus measurement through ambient response method, Springe Trac. Civ. Eng. (2020) 69–98, https://doi.org/10.1007/978-3-030-39738-8_3.
[15] A.M. Matos, J. Granja, S. Nunes, J.L. Barroso-Aguiar, M. Azenha, Hardening characterisation of a non-proprietary and more eco-friendly UHPC, Constr. Build. Mater. 363 (2023) 129803, https://doi.org/10.1016/j.conbuildmat.2022.129803.
[16] S.J. Schmid, L. Zelaya-Lainez, O. Lahayne, M. Peyerl, B.L.A. Pichler, Hourly-Repeated Three-Minutes Creep Testing of a Limestone Calcined Clay Cement Paste (LC3) BT - International RILEM Conference on Synergising Expertise towards Sustainability and Robustness of Cement-based Materials and Concrete Structures, Springer Nature Switzerland, Cham, 2023, pp. 291–299.
[17] L. Cieri, P. Cassese, G. Fabbrocino, A. Occhiuzzi, C. Rainieri, Experimental study about the influence of storage conditions of bulk cement on the early-age stiffness evolution of cementitious pastes, Appl. Sci. 13 (2023), https://doi.org/10.3390/app132111734.
[18] M.A. Oliveira, M. Azenha, P.B. Lourenço, A. Meneghini, E.T. Guimarães, F. Castro, et al., Experimental analysis of carbonation, humidity fields and the evolution of elastic modulus in air lime mortar, Constr. Build. Mater. 416 (2024) 134930, https://doi.org/10.1016/j.conbuildmat.2024.134930.
[19] M. Gupta, I. Go, J. Granja, M. Azenha, T. Ishida, Effect of expansive additives on the early age elastic modulus development of cement paste by ambient response method (ARM), RILEM Book. 31 (2021) 319–327, https://doi.org/10.1007/978-3-030-72921-9_26.
[20] H. Wang, Y. Liu, Z. Hu, Z. Liu, D. Xu, J. Liu, Assessment of determination methods for time-zero of autogenous shrinkage in cement mortars, Cem. Concr. Compos 152 (2024) 105607, https://doi.org/10.1016/j.cemconcomp.2024.105607.
[21] V. Malhotra, N. Carino, Handbook on Nondestructive Testing of Concrete, CRC Press, 2004.
[22] N. Agnes, Determination of E-modulus of young concrete with nondestructive method, J. Mater. Civ. Eng. 9 (1997) 15–20, https://doi.org/10.1061/(ASCE)0899-1561(1997)9:1(15).
[23] R. Aguilar, E. Ramírez, V.G. Haach, M.A. Pando, Vibration-based nondestructive testing as a practical tool for rapid concrete quality control, Constr. Build. Mater. 104 (2016) 181–190, https://doi.org/10.1016/j.conbuildmat.2015.12.053.
[24] B. Delsaute, C. Boulay, J. Granja, J. Carette, M. Azenha, C. Dumoulin, et al., Testing Concrete E-modulus at very early ages through several techniques: an inter-laboratory comparison, Strain 52 (2016) 91–109, https://doi.org/10.1111/str.12172.
[25] T. Russo, R.R. Ribeiro, A. Araghi, R. Lameiras, de, M. Granja, J. Azenha, M. Continuous monitoring of elastic modulus of mortars using a single-board computer and cost-effective components, Buildings 13 (2023), https://doi.org/10.3390/buildings13051117.
[26] R. Rocha Ribeiro, M.I.C. Sousa, J.H. da S. Rêgo, R. de M. Lameiras, Innovative low-cost system for early age E-modulus monitoring of cement pastes: validation and application to nanosilica-added and limestone-calcined clay cements, Mater. Struct. 55 (2022) 13, https://doi.org/10.1617/s11527-021-01849-w.
[27] M. Azenha, J. Silva, J. Granja, A. Gomes-Correia, A Retrospective View of EMM-ARM: application to quality control in soil-improvement and complementary developments, Procedia Eng. 143 (2016) 339–346, https://doi.org/10.1016/j.proeng.2016.06.043.
[28] P. Avitabile, Modal Testing: A Practitioner's Guide, Wiley, 2017.
[29] D.J. Ewins, Modal Testing: Theory, Practice and Application, Wiley, 2000.
[30] L. Wan, X. Xie, L. Wang, P. Li, Q. Huang, Modal analysis of subway tunnel in soft soil during operation, Under Sp. 8 (2023) 181–195, https://doi.org/10.1016/j.undsp.2022.04.008.
[31] R.W. Clough, J. Penzien, Dynamics of Structures, McGraw-Hill, 1975.
[32] GY-61 ADXL335 3-Axis Accelerometer Module Datasheet. 2024.
[33] Raspberry Pi Ltd. Raspberry Pi 3 model B+ Datasheet. 2023.
[34] Analog Devices. ADXL335 Datasheet. 2009.
[35] R.R. Ribeiro, R. de M. Lameiras, Evaluation of low-cost MEMS accelerometers for SHM: frequency and damping identification of civil structures, Lat. Am. J. Solids Struct. (2019) 16, https://doi.org/10.1590/1679-78255308.
[36] Texas Instruments. ADS111x Ultra-Small, Low-Power, I2C-Compatible, 860-SPS, 16-Bit ADCs With Internal Reference, Oscillator, and Programmable Comparator. Dallas, Texas: 2009.
[37] S.V. Modak, Analytical and Experimental Modal Analysis, CRC Press, 2023.
[38] S.P. Timoshenko, J.M. Gere, Theory of Elastic Stability, Dover Publications, 2012.
[39] P. Welch, The use of fast Fourier transform for the estimation of power spectra: a method based on time averaging over short, modified periodograms, IEEE Trans. Audio Electro 15 (1967) 70–73, https://doi.org/10.1109/TAU.1967.1161901.
[40] Rao S.S., Griffin P. Mechanical Vibrations Fifth Edition in SI Units. Sixth Edit. Harlow, United Kingdom: 2011.
[41] I. Pane, W. Hansen, Investigation of blended cement hydration by isothermal calorimetry and thermal analysis, Cem. Concr. Res 35 (2005) 1155–1164, https://doi.org/10.1016/j.cemconres.2004.10.027.
[42] L. PJ, A. RK, G. JMC, J. FK, K. SA, Effect of chemical admixtures on apparent activation energy of cementitious systems, J. Mater. Civ. Eng. 23 (2011) 1654–1661, https://doi.org/10.1061/(ASCE)MT.1943-5533.0000345.
[43] S.J. Siddiqui, K.A. Riding, Effect of calculation methods on cement paste and mortar apparent activation energy, Adv. Civ. Eng. Mater. 1 (2012) 20120011, https://doi.org/10.1520/ACEM20120011.

[44] J. Carette, S. Staquet, Monitoring and modelling the early age and hardening behaviour of eco-concrete through continuous non-destructive measurements: Part II. Mechanical behaviour, Cem. Concr. Compos 73 (2016) 1–9, https://doi.org/10.1016/j.cemconcomp.2016.07.003.
[45] M. Soutsos, F. Kanavaris, A. Hatzitheodorou, Critical analysis of strength estimates from maturity functions, Case Stud. Constr. Mater. 9 (2018) e00183, https://doi.org/10.1016/j.cscm.2018.e00183.
[46] J. Granja, R.R. Ribeiro, T. Russo, R. Lameiras, M. Azenha, Influence of temperature in the early-age elastic modulus evolution of cement pastes and concrete, J. Adv. Concr. Technol. 21 (2023) 803–820, https://doi.org/10.3151/jact.21.803.
[47] Araghi A.M., Ribeiro R.R., Russo T., Granja J.L.D., Azenha M., Lameiras R. de M.. EMM-IRM_Software 2023.
[48] ABNT. NBR 16697: Portland cement - Requirements. Rio de Janeiro: 2018.
[49] ABNT. NBR 7215: Portland cement - Determination of compressive strength. Rio de Janeiro: 2019.
[50] ABNT. NBR NM 43: Portland cement - Determination of the normal consistency paste. Rio de Janeiro: 2003.
[51] BSI, Eurocode 2: Design of Concrete Structures – Part 1-1: General Rules for Buildings, British Standards Institution (BSI), London, UK, 2023.
[52] A.M. Neville. Properties of Concrete, 5th ed., Pearson, Harlow, UK, 2011.
[53] ABNT. NBR 8522: Determination of static modulus of elasticity and deformation by compression. Rio de Janeiro: 2017.
[54] ASTM. C469/C469M-14: Standard Test Method for Static Modulus of Elasticity and Poisson's Ratio of Concrete in Compression. West Conshohocken, United States: 2010.
[55] ASTM. C215: Standard Test Method for Fundamental Transverse, Longitudinal, and Torsional Resonant Frequencies of Concrete Specimens. West Conshohocken, United States: 2008.
[56] Alves H., Otani L.B.. Determination of elastic moduli of concrete by Impulse Excitation Technique. 2022.
[57] LYNX. Lynx Data Acquisition. São Paulo, Brazil: 2004.
[58] PCB. Model 353B01 Accelerometer Kit: Installation and Operating Manual, Rev E. New York, United States: 2011.
[59] PCB. Model 482A22 4-channel, line-powered, ICP sensor signal cond., unity gain, BNC: Installation and Operating Manual. New York, United States: 2015.